# *Ab initio* study of alloying and straining effects on CO interaction with Pt

Muneyuki Tsuda and Hideaki Kasai*
*Department of Applied Physics, Osaka University, Suita, Osaka 565-0871, Japan*
(Received 13 January 2006; published 5 April 2006)

We present the systematic picture of alloying and straining effects on the Pt-CO interaction via *ab initio* density functional calculations. The results show that alloying neighbors (Ru, Sn, and Mo) and/or compressive strain increase the valence electron populations of the Pt atoms in the first layers of the modified Pt surfaces. The larger valence electron population of the Pt atom tends to prevent CO from donating electrons in the adsorption reaction, resulting in the weak Pt-CO bond. We suggest that the degree of the donation from CO determines the Pt-CO bond strength.

DOI: 10.1103/PhysRevB.73.155405 PACS number(s): 68.43.Bc, 82.45.Jn

## I. INTRODUCTION

Polymer electrolyte fuel cells (PEFCs) and their analogous direct methanol fuel cells (DMFCs) are unambiguously designated to be the power-sources for automotive, residential, and portable applications of the future.[1] For both types of fuel cells, platinum is normally used as the anode and cathode catalysts mainly due to its comparatively high catalytic ability and durability. Carbon monoxide (CO) has been known to block the active sites of the Pt surface and lower the catalytic activity. In PEFCs, CO-polluted $H_2$ gas is fed to the Pt anode electrodes if reformate fuel is used. In DMFCs, on the other hand, CO is formed as an intermediate on the Pt anode surfaces. Therefore, how we can readily remove CO from Pt is an important and urgent issue for the stable operation of the fuel cells.

In order to protect from the "CO poisoning," Pt is usually alloyed with a second, or even third, metal element. Ruthenium has been considered to be significantly effective in the CO tolerance of Pt (Ref. 2 and references therein). Tin[3–5] or molybdenum[6–8] has also been known to promote the CO tolerance of Pt as a substitute for the rare and expensive Ru. However, the mechanism by which such alloying metals enhance the CO tolerance of Pt has been debated since the 1970s.[9–14] Two possible mechanisms have been proposed to explain the fact that the alloying metal can improve the CO tolerance of Pt.

One is the "bifunctional mechanism."[9–11] In this mechanism, the alloying metal can dissociate water to form the active oxidant, i.e., a surface hydroxyl intermediate (M-OH). The OH group subsequently oxidizes CO bound to the neighboring Pt, resulting in the low CO coverage. The "bifunctional mechanism" is commonly written as:

$$\text{Pt-CO} + \text{M-OH} \rightarrow \text{Pt} + \text{M} + \text{CO}_2 + \text{H}^+ + \text{e}^-(\text{M:alloying metal}) \qquad (1)$$

This is considered to be the overall reaction paths, though each of the elementary steps has yet to be determined. The active oxygen-containing oxidant has also been proposed as, e.g., O, OH, $H_2O$, or other forms of the adsorbed oxygen.

The other is the "ligand effect."[12–14] In this mechanism, the changes in the electronic structure of Pt by the alloying metal weaken the Pt-CO bond, resulting in the low CO coverage. In order to explain the "ligand effect,"[12–14] the "*d*-band center model"[15,16] is now acceptable, which is a simple two-level model describing the coupling of the CO $5\sigma$ and $2\pi^*$ states to the metal *d* valence states, and is dependent on the position of the *d*-band center relative to the Fermi level. However, the "*d*-band center model"[15,16] is not referred to which of the $5\sigma-d$ and $2\pi^*-d$ couplings is more effective in the metal-CO interaction. We think that further interpretations of the "ligand effect"[12–14] may be encouraged.

In addition to alloying, a current topic in surface modifications has been to tune the surface catalysis by externally straining. The catalytic activities have been observed to noticeably change, e.g., when thin films are strained by either pseudomorphic growth on lattice-mismatched substrates[17,18] or implantation of inert gas bubbles in surfaces.[19,20] Some theoretical groups have confirmed the changes in the CO adsorption energies on strained surfaces.[21–23] In order to interpret the straining effect, the "*d*-band center model"[15,16] has also been adopted,[21,22] indicating that it is relevant to the alloying effect.

It is now generally accepted that periodic slab models can obtain accurate molecular adsorption energies on surfaces. However, theorists encountered a serious problem that most calculations based on the density functional theory (DFT)[24,25] at the generalized gradient approximation (GGA) level using periodic slab models of surfaces cannot correctly reproduce the top-site preference for the CO adsorption on Pt(111).[26–28] Since then, the "puzzle"[26–28] has caused few calculations of the CO/Pt(111) system using periodic slab models within the DFT-GGA. However, the "puzzle"[26–28] is being solved by the cluster-based calculations with hybrid exchange-correlation functionals,[29,30] or by the slab-based calculations with elaborate methodologies.[31–33] We, therefore, think that one of the state-of-the-art methods of today to compute the Pt-CO bond strengths is DFT-based calculations employing hybrid functionals, which describe the highest occupied molecular orbital (HOMO)-lowest unoccupied molecular orbital (LUMO) gap of CO more adequately than the pure functionals.[29,30] To our knowledge, there are several DFT-based calculations on the CO/Pt-based alloy cluster[34–39] and slab[40–42] systems. Ishikawa *et al.*[34–39] for ex-

 

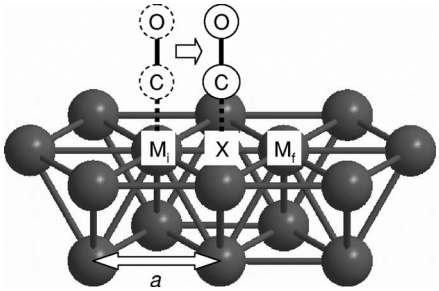


FIG. 1. Schematic representation of the metal surface model constructed by 15 metal atoms, where 10 and 5 atoms are set in the first and second layers, respectively. $M_i$ and $M_f$ denote the positions of the CO-adsorbed metal atoms at the initial and final states, respectively. $X$ denotes the CO position relative to the $M_i$ on the $M_i$-$M_f$ axis. $a$ denotes the lattice constant.

ample, have extensively confirmed a series of the CO adsorption, $CH_3OH$ oxidation and $H_2O$ dissociation on various Pt-based alloy cluster substrates within the framework of the "bifunctional mechanism"[9–11] and "ligand effect."[12–14]

In this article, we systematically investigate the CO interaction with the Pt(111) modified by alloying and straining, in relation to the geometric, vibrational, electronic, and energetic properties, toward more comprehensive understanding of the mechanism for the CO tolerance of Pt.

## II. COMPUTATIONAL PROCEDURES

We first evaluate the CO adsorption on Pt(111), Ru(0001), and Ru(Sn){Mo}-modified Pt(111). We then compare the activation barriers for sliding CO from a metal atom to the nearest neighbor via the bridge site (viz., top-bridge-top path) to systematically consider the CO accessibility to the metal sites. Figure 1 shows the metal surface model constructed by 15 metal atoms, where 10 and 5 atoms are set in the first and second layers, respectively. For all the calculations, the CO axis is fixed perpendicular to the surface, while the surface-C and C-O distances are allowed to relax. $M_i$ and $M_f$ denote the positions of the CO-adsorbed metal atoms at the initial and final states, respectively. $X$ denotes the CO position relative to the $M_i$ on the $M_i$-$M_f$ axis. The previous experimental studies[12,14] showed that alloying effect on the CO electrooxidation significantly exhibits when the alloying metal is present in the first layer of a surface. It can be seen from the previous theoretical studies[38,39] that the position of the alloying metal is not so largely changed as to affect the energetics of reactions. In order to represent the Pt(111) modified by the alloying metals (Ru, Sn, and Mo), therefore, the Pt atom at the $M_f$ in the first layer of the Pt(111) is simply replaced with the corresponding metal atom. A pseudomorphic Sn(Mo) monolayer on Pt(111) [$Sn(Mo)_{ML}/Pt(111)$] is constructed by replacing all the Pt atoms in the first layer with Sn(Mo) atoms for a comparison with the Sn(Mo)-modified Pt(111). The lattice constant ($a$ of Fig. 1) is fixed to that of the bulk [2.77 Å[43] for the Pt(111), Ru(Sn){Mo}-modified Pt(111) and $Sn(Mo)_{ML}/Pt(111)$, and 2.71 Å[43] for the Ru(0001)].

We next evaluate the CO adsorption on strained Pt(111) to discuss the straining effect on the adsorption properties. The strain for Pt(111) is represented by changing the lattice constants ($a$ of Fig. 1) to 2.60 Å for a compressive strain, and conversely to 3.00 Å for a tensile strain, respectively. Moreover, only the position of the Pt atom neighboring to the CO-adsorbed Pt atom is swung to consider the localized strain.

In this study, we mainly allow for the top CO/surface systems because CO tends to adsorb on top of late transition metal surfaces such as Pt(111) and Ru(0001).[44–49] We treat all the systems as non-spin-polarized and preliminarily confirmed that all the surface models are adequate to discuss the above reactions on the realistic nonmagnetic surfaces without any terminal effects depending on the cluster size.

We perform all the calculations based on the density functional theory (DFT)[24,25] with the Becke-Perdew-Wang (B3PW91) hybrid exchange-correlation functional,[50,51] the 6-31G($d,p$) basis set[52] for C and O, and the Hay-Wadt (LANL2DZ) basis set[53–55] for all the metal atoms (Pt, Ru, Sn, and Mo), as implemented in the GAUSSIAN 03 suite of programs.[56] All electron populations are represented using the natural bond orbital (NBO) analysis.[57]

## III. RESULTS AND DISCUSSION

### A. CO adsorption on alloyed Pt(111)

CO tends to molecularly adsorb on Pt(111).[58,59] The CO dissociation may not occur even on the alloyed Pt(111) because Pt is, in fact, considered the main component of the alloyed surfaces due to the possible segregation of the alloying metals. For simplicity, therefore, we preclude the possibility of the CO dissociation. Table I gives the CO adsorption energies, bond distances, and vibrational frequencies of the top CO/Pt(111), CO/Ru(0001), CO/Ru(Sn) {Mo}-modified Pt(111) and $CO/Sn(Mo)_{ML}/Pt(111)$ along with the experimental data if available.[44–49] The predicted bond distances and vibrational frequencies of the top CO/Pt(111) and CO/Ru(0001) are in good agreement with the experimental results.[44–49] Considering the agreement with the experimental results,[44–49] and the large mass-difference between CO and the metals, the allowance to relax the metal atoms may not be so effective. We additionally confirmed the top-site preferences for the CO adsorptions on Pt(111) and Ru(0001).

Neighbored by a Ru atom, the Pt-CO bond is weakened ($E_{ads}$: 1.853 eV → 1.715 eV) due to the "ligand effect."[12–14] Surrounded by Pt atoms, on the other hand, the Ru-CO bond is significantly strengthened ($E_{ads}$: 1.906 eV → 2.472 eV). In the case of the top CO/Sn(Mo)-modified Pt(111), the Pt-CO bond is also weakened [$E_{ads}$: 1.853 eV → 1.729(1.610) eV] due to the "ligand effect."[12–14] However, the Sn(Mo)-CO bond is weaker [$E_{ads}$: 0.368(1.446) eV] than the Pt-CO bond. These trends of the alloying effects by Ru, Sn, and Mo are in good agreement with the previous computational results.[34–37,40,41] However, a pure functional suggests a different tendency of Mo from ours.[42] Our results imply that CO prefers the Ru site of the Ru-modified Pt(111) and the Pt site of the Sn(Mo)-modified Pt(111).

TABLE I. CO adsorption energies $E_{ads}$, bond distances $d$ and vibrational frequencies $\nu$ of the top CO/Pt(111), CO/Ru(0001), CO/Ru(Sn){Mo}-modified Pt(111), and CO/Sn(Mo)$_{ML}$/Pt(111) along with the experimental data if available. (Refs. 44–49). Each of the adsorption energies is relative to the sum of the total energies of the isolated CO and corresponding substrate. M denotes the CO-adsorbed metal atom.

| Surface | Site | $E_{ads}$ [eV] | $d$(M-C) [Å] | $d$(C-O) [Å] | $\nu$(M-C) [cm$^{-1}$] | $\nu$(C-O) [cm$^{-1}$] |
|---|---|---|---|---|---|---|
| Pt(111) | Top Pt | 1.853 | 1.856 | 1.148 | 495 | 2139 |
| Exp. (Ref. 44)[a] | | | 1.85±0.10 | 1.15±0.10 | | |
| Exp. (Ref. 45)[b] | | | | | 470 | 2100 |
| Exp. (Ref. 46)[c] | | | | | 467 | 2104 |
| Ru(0001) | Top Ru | 1.906 | 1.856 | 1.162 | 487 | 2008 |
| Exp. (Ref. 47)[d] | | | 1.93±0.04 | 1.10±0.05 | | |
| Exp. (Ref. 48)[e] | | | | | 445 | 1980–2080 |
| Exp. (Ref. 49)[f] | | | | | 447 | 1990 |
| Ru-modified | Top Pt | 1.715 | 1.857 | 1.149 | 491 | 2135 |
| Pt(111) | Top Ru | 2.472 | 1.848 | 1.155 | 518 | 2073 |
| Sn-modified | Top Pt | 1.729 | 1.861 | 1.148 | 489 | 2136 |
| Pt(111) | Top Sn | 0.368 | 3.150 | 1.134 | 47 | 2238 |
| Mo-modified | Top Pt | 1.610 | 1.866 | 1.149 | 485 | 2133 |
| Pt(111) | Top Mo | 1.446 | 2.067 | 1.146 | 350 | 2093 |
| Sn$_{ML}$/Pt(111) | Top Sn | 0.092 | 3.470 | 1.135 | 52 | 2226 |
| Mo$_{ML}$/Pt(111) | Top Mo | 1.755 | 2.027 | 1.160 | 453 | 2024 |

[a]Low energy electron diffraction (LEED), CO coverage ($\theta_{CO}$)=0.3.
[b]Electron energy loss spectroscopy (EELS), $\theta_{CO}$=0.24.
[c]Reflection absorption infrared spectroscopy (RAIRS), $\theta_{CO}$=0.5.
[d]LEED, $\theta_{CO}$=0.33.
[e]EELS, $\theta_{CO}$=0.07.
[f]RAIRS, $\theta_{CO}$=0.33

In order to clarify the CO preferences, we systematically consider the CO accessibility to the metal sites. Figure 2 show the minimum potential energy curves for the CO/Pt(111), CO/Ru(0001), and CO/Ru(Sn){Mo}-modified Pt(111) as a function of the $M_i$-$X$ distance on the $M_i$-$M_f$ axis (see Fig. 1). In Fig. 2(c), the activation barrier for sliding from Ru to Pt on the Ru-modified Pt(111) is significantly high (1.069 eV) as compared to the Pt→Pt(0.360 eV) on the Pt(111) [see Fig. 2(a)], Ru→Ru(0.349 eV) on the Ru(0001) [see Fig. 2(b)], and Pt→Ru(0.311 eV) on the Ru-modified Pt(111) [see Fig. 2(c)]. In Fig. 2(d), the activation barrier for sliding from Pt to Sn on the Sn-modified Pt(111) is much higher (1.629 eV) than the Sn→Pt(0.269 eV). In Fig. 2(e), the activation barrier for sliding from Pt to Mo on the Mo-modified Pt(111) is also higher (0.323 eV) than the Mo →Pt(0.160 eV). The allowance to tilt CO may lower the activation barriers. However, the significant barriers beyond the differences of the adsorption energies on both metal sites are not involved holding perpendicular to the surface. As a result, the CO accessibility is roughly determined by the differences of the adsorption energies on the both metal sites. Therefore, we have demonstrated that CO tends to localize on the Ru site of the Ru-modified Pt(111) and the Pt site of the Sn(Mo)-modified Pt(111).

Table II gives the atomic charges and electronic configurations of the metal atoms centered in the first layers of the isolated Pt(111), Ru(0001), Ru(Sn){Mo}-modified

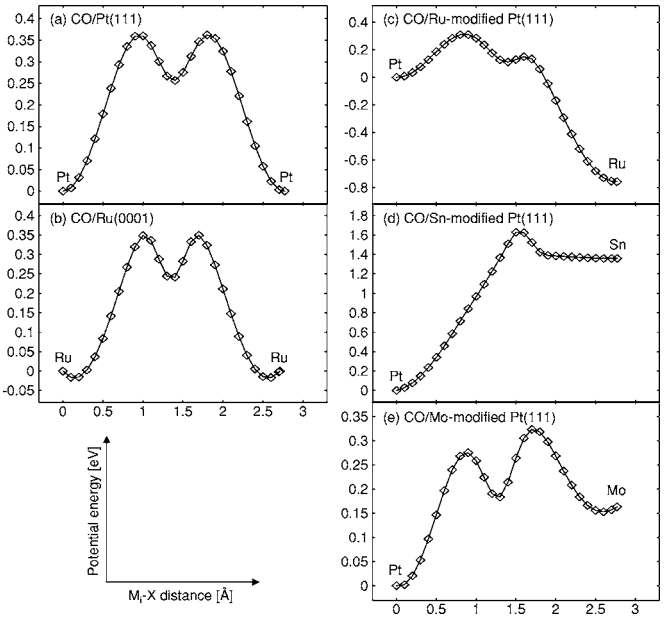


FIG. 2. Minimum potential energy curves for the (a) CO/Pt(111), (b) CO/Ru(0001), (c) CO/Ru-modified Pt(111), (d) CO/Sn-modified Pt(111), and (e) CO/Mo-modified Pt(111) as a function of the $M_i$-$X$ distance on the $M_i$-$M_f$ axis (see Fig. 1), respectively. Each of the minimum potential energies is relative to the total energy of the corresponding top CO-adsorbed substrate.

TABLE II. Atomic charges $q$ and electronic configurations of the metal atoms centered in the first layers of the isolated Pt(111), Ru(0001), Ru(Sn){Mo}-modified Pt(111), and $Sn(Mo)_{ML}$/Pt(111). The values in parentheses are the differences from the electronic configuration of the pristine Pt(111). M denotes the corresponding metal atom.

| Surface | Metal | $q$(M) | Electronic configuration |
|---|---|---|---|
| Pt(111) | Pt | 0.000 | [core] $5d^{9.06}6s^{0.81}6p^{0.05}6d^{0.02}7s^{0.01}7p^{0.06}$ |
| Ru(0001) | Ru | −0.111 | [core] $4d^{7.31}5s^{0.71}5p^{0.03}5d^{0.02}6p^{0.05}$ |
| Ru-modified | Pt | −0.066 | [core] $5d^{9.15}(+0.09)6s^{0.80}(-0.01)6p^{0.05}6d^{0.02}7s^{0.01}7p^{0.05}(-0.01)$ |
| Pt(111) | Ru | −0.061 | [core] $4d^{7.33}5s^{0.61}5p^{0.03}5d^{0.02}6p^{0.07}$ |
| Sn-modified | Pt | −0.146 | [core] $5d^{9.27}(+0.21)6s^{0.76}(-0.05)6p^{0.07}(+0.02)6d^{0.02}7s^{0.01}7p^{0.03}(-0.03)$ |
| Pt(111) | Sn | 0.191 | [core] $5s^{1.25}5p^{2.52}6p^{0.03}$ |
| Mo-modified | Pt | −0.073 | [core] $5d^{9.17}(+0.11)6s^{0.80}(-0.01)6p^{0.05}6d^{0.02}7s^{0.01}7p^{0.05}(-0.01)$ |
| Pt(111) | Mo | 0.030 | [core] $4d^{5.13}5s^{0.66}5p^{0.04}5d^{0.06}6p^{0.08}$ |
| $Sn_{ML}$/Pt(111) | Sn | −0.095 | [core] $5s^{1.19}5p^{2.88}6p^{0.02}$ |
| $Mo_{ML}$/Pt(111) | Mo | −0.143 | [core] $4d^{5.39}5s^{0.67}5p^{0.01}5d^{0.05}6p^{0.04}$ |

Pt(111), and $Sn(Mo)_{ML}$/Pt(111). The degree of the electron transfer between two metal atoms depends on the electronegativity of each metal atom. In the case of the Ru-modified Pt(111), the electron transfer from the Ru atom to the Pt atom occurs because the electronegativities (Pauling scale) of Pt and Ru are 2.28 and 2.20, respectively. As a result, the valence electron population of the Pt atom increases [$q$(Pt):0.000→−0.066]. The weaker Pt-CO bond for the CO/Ru-modified Pt(111) (see Table I) indicates that the larger valence electron population of the Pt atom is less favorable for the CO adsorption. On the other hand, the valence electron population of the Ru atom decreases [$q$(Ru):−0.111→−0.061]. The stronger Ru-CO bond for the CO/Ru-modified Pt(111) (see Table I) indicates that the smaller valence electron population of the Ru atom is more favorable for the CO adsorption. In the case of the Sn-modified Pt(111), the electron transfer from the Sn atom to the Pt atom occurs because the electronegativities (Pauling scale) of Pt and Sn are 2.28 and 1.96, respectively. As a result, the larger electron population [$q$(Pt):0.000→−0.146] of the Pt atom weakens the Pt-CO bond (see Table I) for a similar reason to the Pt-CO bond for the CO/Ru-modified Pt(111). On the other hand, the Sn atom has the fully occupied $d$ orbitals, resulting in the significantly weak Sn-CO bond (see Table I), which is still stronger than the Sn-CO bond for the CO/$Sn_{ML}$/Pt(111) (see Table I). The stronger Sn-CO bond for the CO/Sn-modified Pt(111) (see Table I) indicates that the smaller valence electron population [$q$(Sn):−0.095→0.191] of the Sn atom is more favorable for the CO adsorption for a similar reason to the Ru-CO bond for the CO/Ru-modified Pt(111). In the case of the Mo-modified Pt(111), the electron transfer from the Mo atom to the Pt atom occurs because the electronegativities (Pauling scale) of Pt and Mo are 2.28 and 2.16, respectively. Consequently, the larger electron population [$q$(Pt):0.000→−0.073] of the Pt atom weakens the Pt-CO bond (see Table I) for a similar reason to the Pt-CO bond for the CO/Ru-modified Pt(111). On the other hand, the Mo-CO bond is comparatively weak (see Table I), and moreover is weaker than the Mo-CO bond for the CO/$Mo_{ML}$/Pt(111) (see Table I). The weaker Mo-CO bond for the CO/Mo-modified Pt(111) (see Table I) indicates that the smaller valence electron population [$q$(Mo):−0.143→0.030] of the Mo atom is less favorable for the CO adsorption, which is reverse to the other metal-CO bonds.

Based on our results, we provide the following scenario as a possible mechanism for the CO tolerance of Pt by Ru, Sn, and Mo. There is supposed to be both the Pt and alloying metal sites in the alloyed Pt surfaces. When CO contained in $H_2$ gas adsorbs on the Ru-modified Pt surface, the Pt sites tend to be free from CO, and thus activate $H_2$ even in the presence of CO because CO on the Pt site tends to move to the Ru site. On the other hand, CO on the Ru site tends to be readily oxidized to $CO_2$ with an oxygen-containing species on the surface.[60,61] When CO moving from the Pt site toward the Ru site is oxidized with the oxygen-containing species on the Ru site, the mechanism is rationalized in terms of the "bifunctional mechanism."[9–11] On the Sn-modified and Mo-modified Pt surfaces, however, CO tends to localize on the Pt sites and, therefore, be oxidized with the oxygen-containing species on the alloying metal site depending on the "bifunctional mechanism"[9–11] as experimentally observed.[3–8] Unlike CO, OH which is a possible oxygen-containing species tends to strongly adsorb on various metals.[35–39,41,42] On the whole, we think that independence from the "bifunctional

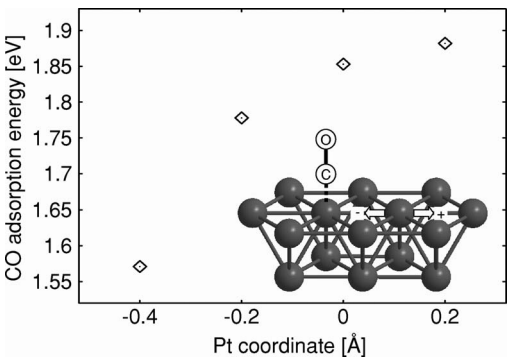


FIG. 3. CO adsorption energies on the localized-strained Pt(111) as a function of the coordinate of the neighboring Pt atom at the $M_f$ along the $M_i$-$M_f$ axis relative to the original position, where the $M_i$ side corresponds to minus (see Fig. 1 and the inset in this figure).

TABLE III. CO adsorption energies $E_{ads}$, bond distances $d$ and vibrational frequencies $\nu$ of the top CO/Pt(111) as a function of the lattice constant $a$ (see Fig. 1). Each of the adsorption energies is relative to the sum of the total energies of the isolated CO and corresponding substrate.

| $a$ [Å] | $E_{ads}$ [eV] | $d$(Pt-C) [Å] | $d$(C-O) [Å] | $\nu$(Pt-C) [cm$^{-1}$] | $\nu$(C-O) [cm$^{-1}$] |
|---|---|---|---|---|---|
| 2.60 | 1.309 | 1.885 | 1.147 | 462 | 2142 |
| 2.77 (bulk) | 1.853 | 1.856 | 1.148 | 495 | 2139 |
| 3.00 | 2.313 | 1.817 | 1.150 | 549 | 2141 |

mechanism"[9–11] in the removal of CO from Pt may be a possible reason why the well-known Ru is comparatively effective in the CO tolerance of Pt (Ref. 2 and references therein).

### B. CO adsorption on strained Pt(111)

Table III gives the CO adsorption energies, bond distances, and vibrational frequencies of the top CO/Pt(111) as a function of the lattice constant ($a$ of Fig. 1). The Pt-CO bond is weakened ($E_{ads}$: 1.853 eV $\rightarrow$ 1.309 eV) as the lattice constant decreases, and vice versa ($E_{ads}$: 1.853 eV $\rightarrow$ 2.313 eV). This trend is similar to that of the CO/Ru(0001) by Mavrikakis *et al.*[21]

Table IV gives the atomic charges and electronic configurations of the Pt atoms centered in the first layers of the isolated Pt(111) as a function of the lattice constant. The valence electron population of the Pt atom increases [$q$(Pt): 0.000 $\rightarrow$ −0.072] as the lattice constant decreases, and vice versa [$q$(Pt): 0.000 $\rightarrow$ 0.021]. As a result, the larger valence electron population of the Pt atom weakens the Pt-CO bond, and vice versa. This trend is in good agreement with that of the alloying effect on the Pt-CO interaction as shown in Sec. III A. Therefore, we have demonstrated that the larger (smaller) valence electron population in the compressive-strained (tensile-strained) Pt(111) tends to repel (attract) CO. Note that this relation to the straining effect is not always true for other metals as pointed out by Pala *et al.*[23] The relation may be reversed for the metals with the originally small $d$ electron populations such as Mo, which is implied in Sec. III A.

In order to consider the localized strain for Pt(111), we vary only the position of the neighboring Pt atom at the $M_f$ along the $M_i$-$M_f$ axis (see Fig. 1). Figure 3 shows the CO adsorption energies as a function of the coordinate of the neighboring Pt atom at the $M_f$ along the $M_i$-$M_f$ axis relative to the original position, where the $M_i$ side corresponds to minus (see Fig. 1 and the inset in Fig. 3). In Fig. 3, the Pt-CO bond tends to be weakened as the neighboring Pt atom approaches the CO-adsorbed Pt atom, and vice versa. Therefore, it can be seen that the specific straining effect qualitatively supports the above dependence of the Pt-CO bond strength on the lattice constant.

### C. Underlying factor determining CO interaction with Pt

In the CO adsorption on a metal surface, the metal-CO bond strength depends on both the donation (from the bonding orbitals of the CO to the antibonding orbitals of the metal) and the back-donation (from the bonding orbitals of the metal to the antibonding orbitals of the CO).[62] In particular, the metal-C and C-O bond strengths strongly depend on the donation and back-donation, respectively.

Figure 4 (5) shows the CO adsorption energies on the Pt(111) considered in this study as functions of the Pt-C and C-O distances (stretching frequencies), respectively. In Fig. 4, the Pt-CO bond tends to be weakened as the Pt-C distance is long, and vice versa. On the other hand, the Pt-CO bond strength does not strongly correlate with the C-O distance. Moreover, the C-O distance is hardly changed. In Fig. 5, the Pt-CO bond tends to be weakened as the Pt-C stretching frequency decreases, and vice versa. On the other hand, the Pt-CO bond strength does not strongly correlate with the C-O stretching frequency. Moreover, the C-O stretching frequency is hardly changed. This trend agrees with the suggestion by Wasileski *et al.*[63] that there is no clear-cut relationship between the metal-C and C-O stretching frequencies for the CO/Pt-group (111). Our results indicate that the Pt-C bonding is more dominant to the Pt-CO bond strength than the C-O bonding. Therefore, we have demonstrated that the degree of the donation from CO is more effective in the Pt-CO bond strength than that of the back-donation to CO.

On the Pt-C sides of Figs. 4 and 5, the Pt-CO bond strength tends to be weakened as the valence electron population of the Pt atom in the first layer of the Pt surface increases, and vice versa. This indicates that the donation tends to decrease as the valence electron population of the Pt atom in the first layer of the Pt surface increases, and vice versa.

TABLE IV. Atomic charges $q$ and electronic configurations of the Pt atoms centered in the first layers of the isolated Pt(111) as a function of the lattice constant $a$ (see Fig. 1). The values in parentheses are the differences from the electronic configuration of the pristine Pt(111).

| $a$ [Å] | $q$(Pt) | Electronic configuration |
|---|---|---|
| 2.60 | −0.072 | [core] $5d^{9.10}(+0.04)6s^{0.82}(+0.01)6p^{0.11}(+0.06)6d^{0.02}7s^{0.01}7p^{0.03}(-0.03)$ |
| 2.77 (bulk) | 0.000 | [core] $5d^{9.06}6s^{0.81}6p^{0.05}6d^{0.02}7s^{0.01}7p^{0.06}$ |
| 3.00 | 0.021 | [core] $5d^{9.11}(+0.05)6s^{0.79}(-0.02)6p^{0.04}(-0.01)6d^{0.01}(-0.01)7s^{0.01}7p^{0.03}(-0.03)$ |

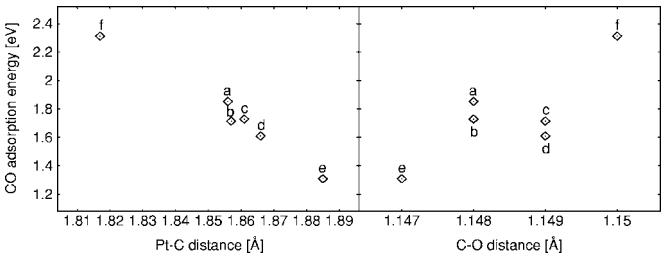


FIG. 4. CO adsorption energies on the Pt(111) [(a) Pt(111), (b) Ru-modified Pt(111), (c) Sn-modified Pt(111), (d) Mo-modified Pt(111), (e) Pt(111) ($a$=2.60 Å), and (f) Pt(111) ($a$=3.00 Å)] as functions of the Pt-C and C-O distances, respectively.

However, this trend is reversed in the case of the Mo-CO bond strength as implied in Secs. III A and III B. Figure 6 shows the highest occupied molecular orbitals (HOMOs) and lowest unoccupied molecular orbitals (LUMOs) of the isolated Pt(111), Mo-modified Pt(111), and $Mo_{ML}$/Pt(111). In Fig. 6, both energies of the HOMO (−5.709 eV) and LUMO (−5.166 eV) of the isolated Pt(111) are significantly low, which is in good agreement with the experimental work function (~5.7 eV) of Pt, and are shifted up as the proportion of Mo increases. This indicates that the back-donation from Mo is more favorable due to the smaller energy-difference from the LUMO (−0.614 eV) of CO. Comparing the CO/Mo-modified Pt(111) (Mo site) with the CO/$Mo_{ML}$/Pt(111), the C-O distance (stretching frequency) is explicitly changed from 1.160 Å (2024 $cm^{-1}$) to 1.146 Å (2093 $cm^{-1}$) (see Table I). This indicates that the back-donation is effective in the Mo-CO bond strength. Therefore, the reversed trend may be attributed to the decreased back-donation from the smaller $d$ electron population of the Mo atom. Figure 7 shows the CO adsorption energies on the Pt(111) considered in this study as a function of the 5$d$ orbital population of the Pt atom centered in the first layer of the isolated Pt(111). In Fig. 7, the Pt-CO bond strength tends to be weakened as the Pt(5$d$) orbital population increases when the difference from the electronic configuration of the pristine Pt(111) is mainly due to the 5$d$ electrons, i.e., in the case of the Ru(Mo)-modified Pt(111) (see Table II). However, the Pt-CO bond strength does not strongly correlate with the Pt(5$d$) orbital population, and the electrons from CO tend to be donated to other valence orbitals of the Pt when the alloying neighbor has no $d$ electrons in the valence electrons, i.e., in the case of the Sn-modified Pt(111) (see Table II), and when the surface is in the energetically excited state, i.e., in the case of the strained Pt(111) (see Table IV).

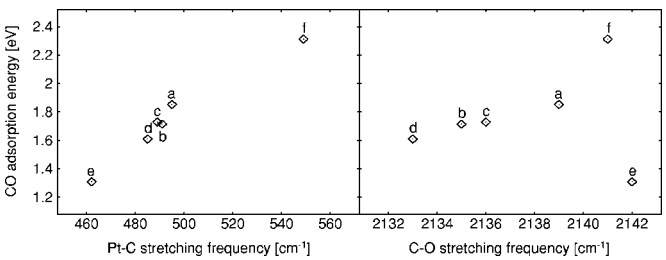


FIG. 5. CO adsorption energies on the Pt(111) [(a) Pt(111), (b) Ru-modified Pt(111), (c) Sn-modified Pt(111), (d) Mo-modified Pt(111), (e) Pt(111) ($a$=2.60 Å), and (f) Pt(111) ($a$=3.00 Å)] as functions of the Pt-C and C-O stretching frequencies, respectively.

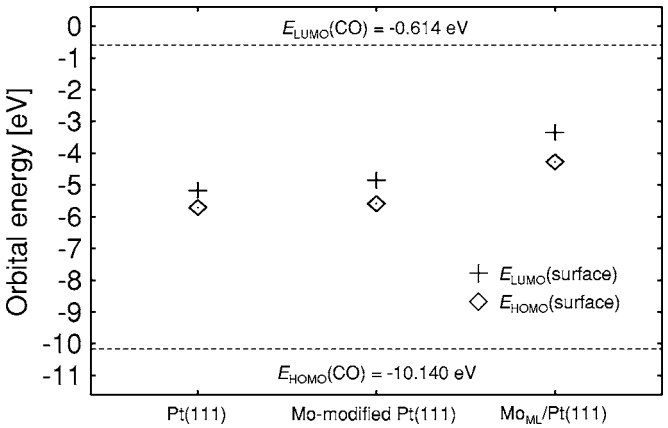


FIG. 6. Energies of the highest occupied molecular orbitals (HOMOs) and lowest unoccupied molecular orbitals (LUMOs) of the isolated Pt(111), Mo-modified Pt(111) and $Mo_{ML}$/Pt(111). Energies of the HOMO and LUMO of CO are also shown by the broken lines.

## IV. CONCUDING REMARKS

We systematically confirmed the role of alloying and straining in the Pt-CO interaction. The results show that alloying neighbors (Ru, Sn, and Mo) and/or compressive strain increase the valence electron populations of the Pt atoms in the first layers of the modified Pt surfaces. Consequently, the effect tends to decrease the donation from CO in the adsorption reaction, resulting in the weak Pt-CO bond. We demonstrated that the Pt-CO bond strength strongly depends on the Pt-C bonding and, therefore, concluded that the degree of the donation determines the Pt-CO bond strength.

## ACKNOWLEDGMENTS

This work was partially supported by the 21st Century COE program (G18) from the Japan Society for the Promo-

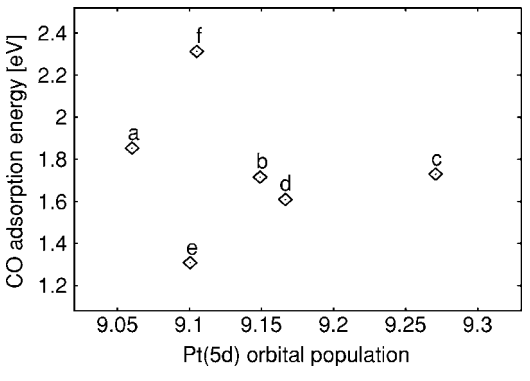


FIG. 7. CO adsorption energies on the Pt(111) [(a) Pt(111), (b) Ru-modified Pt(111), (c) Sn-modified Pt(111), (d) Mo-modified Pt(111), (e) Pt(111) ($a$=2.60 Å), and (f) Pt(111) ($a$=3.00 Å)] as a function of the 5$d$ orbital population of the Pt atom centered in the first layer of the isolated Pt(111).

tion of Science (JSPS), the Research and Development of Polymer Electrolyte Fuel Cell Systems from the New Energy and Industrial Technology Development Organization (NEDO), and a Grant-in-Aid for Scientific Research on Priority Areas (Developing Next Generation Quantum Simulators and Quantum-Based Design Techniques) by the Ministry of Education, Culture, Sports, Science and Technology (MEXT). All the computations were done using the facilities of the Japan Atomic Energy Agency (JAEA) and the Cybermedia Center, Osaka University (CMC).

*Electronic address: kasai@dyn.ap.eng.osaka-u.ac.jp

[1] B. C. H. Steele and A. Heinzel, Nature (London) **414**, 345 (2001).
[2] F. Maillard, G. Q. Lu, A. Wieckowski, and U. Stimming, J. Phys. Chem. B **109**, 16230 (2005).
[3] B. E. Hayden, M. E. Rendall, and O. South, J. Am. Chem. Soc. **125**, 7738 (2003).
[4] S. Tillmann, G. Samjeské, K. A. Friedrich, and H. Baltruschat, Electrochim. Acta **49**, 73 (2003).
[5] M. Arenz, V. Stamenkovic, B. B. Blizanac, K. J. Mayrhofer, N. M. Markovic, and P. N. Ross, J. Catal. **232**, 402 (2005).
[6] G. Samjeské, H. Wang, T. Löffler, and H. Baltruschat, Electrochim. Acta **47**, 3681 (2002).
[7] S. Mukerjee, R. C. Urian, S. J. Lee, E. A. Ticianelli, and J. McBreen, J. Electrochem. Soc. **151**, A1094 (2004).
[8] S. Zafeiratos, G. Papakonstantinou, M. M. Jacksic, and S. G. Neophytides, J. Catal. **232**, 127 (2005).
[9] M. Watanabe and S. Motoo, J. Electroanal. Chem. Interfacial Electrochem. **60**, 267 (1975).
[10] H. A. Gasteiger, N. Marković, P. N. Ross, Jr., and E. J. Cairns, J. Phys. Chem. **97**, 12020 (1993).
[11] R. Ianniello, V. M. Schmidt, U. Stimming, J. Stumper, and A. Wallau, Electrochim. Acta **39**, 1863 (1994).
[12] J. C. Davies, B. E. Hayden, and D. J. Pegg, Electrochim. Acta **44**, 118 (1998).
[13] F. B. de Mongeot, M. Scherer, B. Gleich, E. Kopatzki, and R. J. Behm, Surf. Sci. **411**, 249 (1998).
[14] J. C. Davies, B. E. Hayden, and D. J. Pegg, Surf. Sci. **467**, 118 (2000).
[15] B. Hammer, Y. Morikawa, and J. K. Nørskov, Phys. Rev. Lett. **76**, 2141 (1996).
[16] B. Hammer and J. K. Nørskov, Adv. Catal. **45**, 71 (2000).
[17] E. Kampshoff, E. Hahn, and K. Kern, Phys. Rev. Lett. **73**, 704 (1994).
[18] R. Otero, F. Calleja, V. M. García-Suárez, J. J. Hinarejos, J. de la Figuera, J. Ferrer, A. L. Vázquez de Parga, and R. Miranda, Surf. Sci. **550**, 65 (2004).
[19] M. Gsell, P. Jakob, and D. Menzel, Science **280**, 717 (1998).
[20] P. Jakob, M. Gsell, and D. Menzel, J. Chem. Phys. **114**, 10075 (2001).
[21] M. Mavrikakis, B. Hammer, and J. K. Nørskov, Phys. Rev. Lett. **81**, 2819 (1998).
[22] A. Schlapka, M. Lischka, A. Groß, U. Kräsberger, and P. Jakob, Phys. Rev. Lett. **91**, 016101 (2003).
[23] R. G. S. Pala and F. Liu, J. Chem. Phys. **120**, 7720 (2004).
[24] P. Hohenberg and W. Kohn, Phys. Rev. **136**, B864 (1964).
[25] W. Kohn and L. J. Sham, Phys. Rev. **140**, A1133 (1965).
[26] P. J. Feibelman, B. Hammer, J. K. Nørskov, F. Wagner, M. Scheffler, R. Stumpf, R. Watwe, and J. Dumesic, J. Phys. Chem. B **105**, 4018 (2001).
[27] I. Grinberg, Y. Yourdshahyan, and A. M. Rappe, J. Chem. Phys. **117**, 2264 (2002).
[28] R. A. Olsen, P. H. T. Philipsen, and E. J. Baerends, J. Chem. Phys. **119**, 4522 (2003).
[29] A. Gil, A. Clotet, J. M. Ricart, G. Kresse, M. García-Hernández, N. Rösch, and P. Sautet, Surf. Sci. **530**, 71 (2003).
[30] K. Doll, Surf. Sci. **573**, 464 (2004).
[31] G. Kresse, A. Gil, and P. Sautet, Phys. Rev. B **68**, 073401 (2003).
[32] H. Orita, N. Itoh, and Y. Inada, Chem. Phys. Lett. **384**, 271 (2004).
[33] S. E. Mason, I. Grinberg, and A. M. Rappe, Phys. Rev. B **69**, 161401(R) (2004).
[34] R. C. Binning, M. S. Liao, C. R. Cabrera, Y. Ishikawa, H. Iddir, R. Liu, E. S. Smotkin, A. J. Aldykiewicz, Jr., and D. J. Myers, Int. J. Quantum Chem. **77**, 589 (2000).
[35] M. S. Liao, C. R. Cabrera, and Y. Ishikawa, Surf. Sci. **445**, 267 (2000).
[36] Y. Ishikawa, M. S. Liao, and C. R. Cabrera, Surf. Sci. **463**, 66 (2000).
[37] Y. Ishikawa, M. S. Liao, and C. R. Cabrera, Surf. Sci. **513**, 98 (2002).
[38] Y. Ishikawa, R. R. Diaz-Morales, A. Perez, M. J. Vilkas, and C. R. Cabrera, Chem. Phys. Lett. **411**, 404 (2005).
[39] A. Perez, M. J. Vilkas, C. R. Cabrera, and Y. Ishikawa, J. Phys. Chem. B **109**, 23571 (2005).
[40] Q. Ge, S. Desai, M. Neurock, and K. Kourtakis, J. Phys. Chem. B **105**, 9533 (2001).
[41] M. T. M. Koper, T. E. Shubina, and R. A. van Santen, J. Phys. Chem. B **106**, 686 (2002).
[42] T. E. Shubina and M. T. M. Koper, Electrochim. Acta **47**, 3621 (2002).
[43] C. Kittel, *Introduction to Solid State Physics*, 7th ed. (Wiley, New York, 1996).
[44] G. S. Blackman, M. L. Xu, D. F. Ogletree, M. A. Van Hove, and G. A. Somorjai, Phys. Rev. Lett. **61**, 2352 (1988).
[45] H. Steininger, S. Lehwald, and H. Ibach, Surf. Sci. **123**, 264 (1982).
[46] M. Tüshaus, D. Hoge, and A. M. Bradshaw, Surf. Sci. **213**, 49 (1989).
[47] H. Over, W. Moritz, and G. Ertl, Phys. Rev. Lett. **70**, 315 (1993).
[48] G. E. Thomas and W. H. Weinberg, J. Chem. Phys. **70**, 954 (1979).
[49] P. Jakob and B. N. J. Persson, Phys. Rev. Lett. **78**, 3503 (1997).
[50] A. D. Becke, J. Chem. Phys. **98**, 5648 (1993).
[51] J. P. Perdew and Y. Wang, Phys. Rev. B **45**, 13244 (1992).
[52] P. C. Hariharan and J. A. Pople, Theor. Chim. Acta **28**, 213 (1973).
[53] P. J. Hay and W. R. Wadt, J. Chem. Phys. **82**, 270 (1985).
[54] W. R. Wadt and P. J. Hay, J. Chem. Phys. **82**, 284 (1985).
[55] P. J. Hay and W. R. Wadt, J. Chem. Phys. **82**, 299 (1985).

[56] M. J. Frisch *et al.*, Gaussian 03, Revision B.05, Gaussian, Inc., Pittsburgh PA, 2003.
[57] A. E. Reed, L. A. Curtiss, and F. Weinhold, Chem. Rev. (Washington, D.C.) **88**, 899 (1988).
[58] G. BrodÉn, T. N. Rhodin, C. Brucker, R. Benbow, and Z. Hurych, Surf. Sci. **59**, 593 (1976).
[59] Y. Morikawa, J. J. Mortensen, B. Hammer, and J. K. Nørskov, Surf. Sci. **386**, 67 (1997).
[60] W. F. Lin, J. M. Jin, P. A. Christensen, and K. Scott, Electrochim. Acta **48**, 3815 (2003).
[61] J. M. Jin, W. F. Lin, and P. A. Christensen, J. Electroanal. Chem. **563**, 71 (2004).
[62] G. Blyholder, J. Phys. Chem. **68**, 2772 (1964).
[63] S. A. Wasileski, M. T. M. Koper, and M. J. Weaver, J. Phys. Chem. B **105**, 3518 (2001).